

# Fast bonding $\alpha$ -SiAlON ceramics by spark plasma sintering

Liu Limeng<sup>a,\*</sup>, Ye Feng<sup>a</sup>, Zhou Yu<sup>a</sup>, Zhang Zhiguo<sup>b</sup>, Hou Qinglong<sup>a</sup>

<sup>a</sup> School of Materials Science and Engineering, Harbin Institute of Technology, Xidazhi Street 92, Nangang, Harbin 150001, China

<sup>b</sup> Department of Physics, Harbin Institute of Technology, Harbin 150001, China

Received 22 November 2009; received in revised form 2 May 2010; accepted 16 May 2010

Available online 9 June 2010

## Abstract

Yb- and Y-doped  $\alpha$ -SiAlON ceramics were effectively bonded by spark plasma sintering in less than 20 min without using any interlayer materials at 1650–1700 °C. The microstructures and mechanical properties of the joints were investigated by means of SEM, STEM, EDX, and three-point bending tests. The results showed that  $\alpha$ -SiAlON joint formation was accompanied by fundamental rare earth diffusion. The intergranular liquids in the  $\alpha$ -SiAlON ceramics at the bonding temperatures provided the diffusion paths for the species.  $\alpha$ -SiAlON grain growth across the joining interfaces modified the joint microstructures to secure high bonding strength.

© 2010 Elsevier Ltd. All rights reserved.

**Keywords:** SiAlON; Joining; Spark plasma sintering

## 1. Introduction

$\alpha$ -SiAlON is a solid solution based on  $\alpha$ -Si<sub>3</sub>N<sub>4</sub>.<sup>1</sup> It is generally described by the formula  $RE_{m/v}Si_{12-(m+n)}Al_{m+n}O_nN_{16-n}$ . During the  $\alpha$ -SiAlON formation, Al substitutes for Si and O for N in the  $\alpha$ -Si<sub>3</sub>N<sub>4</sub>, and simultaneously some metal cations ( $RE^{v+}$ ) are incorporated into the  $\alpha$ -Si<sub>3</sub>N<sub>4</sub> structure.  $\alpha$ -SiAlON ceramics are attractive structural materials due to their good room and high temperature mechanical properties, excellent tribological properties, excellent wear resistance, and very good corrosion and oxidation resistance.<sup>2</sup> The application of  $\alpha$ -SiAlON ceramics includes cutting tools and hot-section components for advanced turbines.<sup>2</sup>

In tool making and component preparation, ceramic joining is occasionally demanded and the related research has attracted extensive interests in the last years. The low self-diffusion coefficient of the covalent Si–N bond has led to the application of metallic<sup>3–7</sup> or non-metallic<sup>8–10</sup> interlayers to joint silicon nitride. The so-called diffusion bonding of silicon nitride in the literature actually also includes these kinds of interlayers<sup>3–5</sup> and the joining processes are usually performed at a proper temper-

ature under pressure for rather long holding times even up to hours.<sup>4,5,7,9,10</sup> The diffusion bonding in those literature refers to the transport of the silicon and nitrogen species to form the joints. There are intrinsic disadvantages<sup>3,4,7,8</sup> such as large residual stresses and low service temperature (<800 °C)<sup>7–10</sup> for such diffusion bond joints.

Silicon nitride and the related  $\alpha$ -SiAlON ceramics are practically densified with various sintering aids.<sup>11,12</sup> In the case of  $\alpha$ -SiAlON, transient sintering liquids help to form the self-toughening microstructures.<sup>12</sup> Upon cooling, certain amount of the sintering liquids remains as the various intergranular phases. The compositions of these rare earth rich oxynitride glasses have been successfully used to join Si<sub>3</sub>N<sub>4</sub>-based ceramics.<sup>8–10,13</sup> However in an ideal speculation, if diffusion of these inherent intergranular phase constituents is sufficiently activated,<sup>9</sup> the use of solders to form  $\alpha$ -SiAlON joints may be totally unnecessary.

This paper demonstrated the feasibility of connecting  $\alpha$ -SiAlON ceramics based on the above-mentioned new concept without using any extra-induced interlayer materials. Strong seamless joints<sup>13,14</sup> were obtained by spark plasma sintering (SPS). To the authors' knowledge, experimental works devoted to direct diffusion bonding of silicon nitride or SiAlONs without usage of interlayers are limited. SPS is a new method to consolidate metals, ceramics, and polymers in a very short time as a few

\* Corresponding author. Tel.: +86 451 86413921; fax: +86 451 86413922.  
E-mail address: [liulimeng@hit.edu.cn](mailto:liulimeng@hit.edu.cn) (L. Liu).

minutes.<sup>15</sup> In this study the rapid heating and cooling rates of SPS were also proven efficient in bonding  $\alpha$ -SiAlON ceramics. Seamless joints with bending strength approaching that of the parent materials were obtained in only a few minutes.

## 2. Experimental

The  $\alpha$ -SiAlON composition in this study was  $m = 1.2$ ,  $n = 1.2$  in the general formula  $RE_{m/3}Si_{12-(m+n)}Al_{m+n}O_nN_{16-n}$  (RE = Y, Yb). This composition locates in the single  $\alpha$ -SiAlON phase field.<sup>12,16</sup> Two  $\alpha$ -SiAlON materials, doped respectively with the same amount of Y and Yb, were coupled to form the joints in order to facilitate microstructural observation and analysis of the  $\alpha$ -SiAlON joints. This was because the large elemental number difference between Y and Yb can produce clearer back-scattered electron imaging contrast, and diffusion profiles of the rare earths across the joint interfaces are easier to portray by tracing the elements. The parent  $\alpha$ -SiAlON ceramics were synthesized by SPS. Starting powders for the  $\alpha$ -SiAlON were  $\alpha$ -Si<sub>3</sub>N<sub>4</sub> (E10 Grade, UBE Industries Ltd., Japan), Al<sub>2</sub>O<sub>3</sub> (Grade A16SG, Alcoa), AlN (grade C, H.C. Stark, Berlin, Germany), Y<sub>2</sub>O<sub>3</sub> and Yb<sub>2</sub>O<sub>3</sub> (grade fine, H.C. Stark). When calculating the overall composition, 2.38 wt% SiO<sub>2</sub> and 1.83 wt% Al<sub>2</sub>O<sub>3</sub> (according to the manufacturers' specifications) on the surface of Si<sub>3</sub>N<sub>4</sub> and AlN powders were taken into account.

The powder mixtures were wet-blended for 12 h in isopropanol using Si<sub>3</sub>N<sub>4</sub> balls as the milling media. The slurries were dried and then passed through a 120 mesh sieve. 8 g of each powder mixture batch was loaded into the graphite die with an inner diameter of  $\Phi$  18.5 mm and then was set into the SPS furnace (Dr. Sinter 1080 Sumitomo Coal Mining Company, Ltd.). 0.1 MPa nitrogen was used as a sintering atmosphere. After 5 MPa uniaxial pressure was applied, the loaded die was automatically heated to 700 °C in 4 min. The pressure increased linearly to 20 MPa at the same time. Then the temperature was further raised to 1730 °C at 100 °C/min and to 1750 °C in another 1 min to avoid over-heating. After holding for 10 min, the SPS pressure was released and the power shut off. The average cooling rate was  $\sim$ 300 °C/min down to 700 °C. The heating procedure was monitored by a digital pyrometer focused on the die surface.

Both basal planes of the as-sintered  $\alpha$ -SiAlON cylinders ( $\sim$ 9 mm in height) were ground by a polymer-bonded diamond wheel (120 grits) to remove surface contamination. Diameter of the  $\alpha$ -SiAlON cylinder was reduced to  $\Phi$  18.3 mm by machining to fit the  $\Phi$  18.5 mm die for joining. Further polish of the surfaces to be jointed (which was usually considered indispensable for high quality diffusion joints in the literature<sup>3–5,9,10,13,14</sup>), was not performed in this study. After being ultrasonicated for 10 min in an acetone bath, a Y-SiAlON piece and an Yb-SiAlON piece was assembled in the SPS die for joining. The joining conditions were 1600–1700 °C in a 0.1 MPa nitrogen atmosphere for 0–20 min. The constant SPS pressure covering heating and holding time but released upon cooling was 20 MPa. The heating control and pressure control were the same as sintering the parent  $\alpha$ -SiAlON ceramics. Some selected  $\alpha$ -SiAlON joints were

heat-treated at 1700 °C for 30–120 min in a 0.1 MPa nitrogen atmosphere in a gas-pressing, using a heating rate of 20 °C/min and free cooling.

The samples were sectioned longitudinally, machined, and then polished. The  $\alpha$ -SiAlON grain morphologies were exposed by removing the intergranular phase in molten NaOH if necessary. The densities of the  $\alpha$ -SiAlON ceramics before and after SPS joining were measured by the Archimedes' principle in distilled water at 20 °C. Three-point bend strength was measured at room temperature on an Instron-1196 machine using 1.0 mm  $\times$  2.5 mm  $\times$  16.0 mm specimens with a span of 10.0 mm and a thickness of 1.0 mm. The samples were carefully aligned to make sure the joint seams were right under the crosshead. Eight pieces from different sections of the joint were tested for each condition. Hardness measurements were carried out on polished specimens on a universal hardness tester using a 5 kg load. Fracture toughness was calculated employing the equation of Anstis et al.<sup>17</sup> by assuming the elastic modulus of 300 GPa for both Y- and Yb-SiAlON materials. Microstructural characterization was accomplished with X-ray diffraction (XRD, RIGAKU D/MAX-2200 X-ray diffractometer using copper K $\alpha$  radiation), scanning electron microscopy (SEM; Hitachi S-3500N, Japan), energy dispersive spectrometry (EDS), and scanning transmission electron microscopy (STEM; HAADF-TEM, Model TECNAI G2 F30, FEI Co., The Netherlands). Possible defects in the joints were also examined by observing the fracture surfaces.

## 3. Results and discussion

### 3.1. The joint formation

In synthesis process of the  $\alpha$ -SiAlON materials, the fast heating rate of SPS pushes the SiAlON reaction off equilibrium, avoiding the various solid intermediate phases that always present in hot pressing process to favor both the densification and the dynamic formation of the  $\alpha$ -SiAlONs.<sup>18</sup> Dense single phase Y- and Yb-doped  $\alpha$ -SiAlON ceramics are achieved. Our research results indicate SPS at 1600 °C cannot yield sufficient SiAlON joints in spite of the fact that the eutectic temperature of the SiAlON intergranular phases is  $<1300$  °C<sup>11–13</sup> and plastic deformation in  $\alpha$ -SiAlON ceramics happens around 1550 °C.<sup>10,19–21</sup> Even prolonging the joining time to 20 min at 1600 °C, the resultant joints are still weak and often fail when being sectioned for mechanical property tests.

Joints with satisfying strength are only produced at  $\geq 1650$  °C. The joint formation processes are reflected by the SPS ram displacement as shown in Fig. 1(a). The thermal expansion of the punch, graphite die and the SiAlON couples in the heating stage produced the slope below 1500 °C. The curvature change and the subsequent noticeable shrinkage at the higher temperature, i.e. 1600–1700 °C suggest the occurrence of a small amount of plastic deformation<sup>22</sup> of the SiAlON couples under the 20 MPa unidirectional compressive SPS stress. This plastic deformation should result from grain sliding and grain rearrangement.<sup>19,20</sup> Apparently the plastic deformation takes place at a temperature higher than the eutectic temperature of the RESiAlON intergranular glassy phases. The eutectic reaction

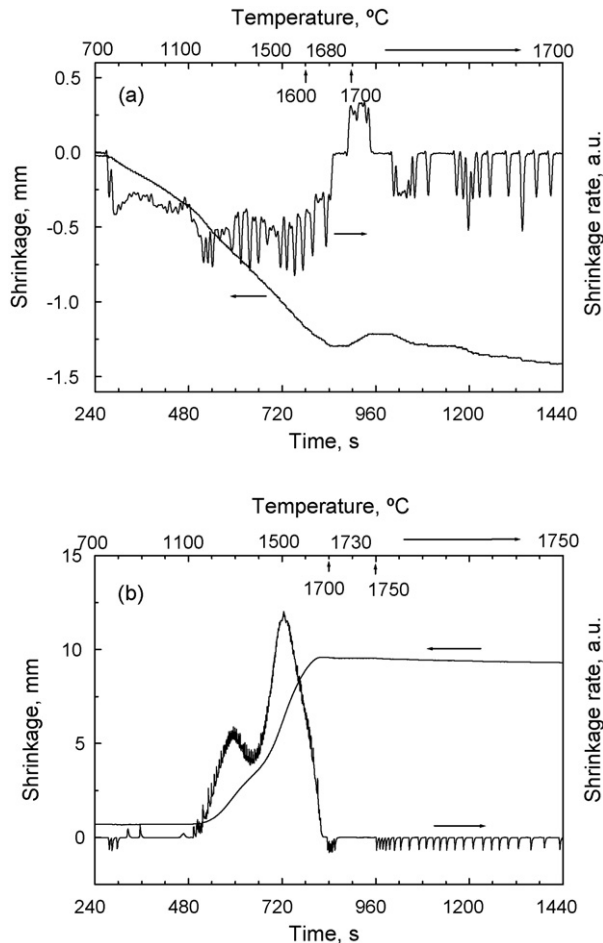


Fig. 1. SPS punch displacement curves, showing (a) deformation of the SiAlON couple during joining, and (b) densification process of the Y-doped  $\alpha$ -SiAlON.

between the  $\text{SiO}_2$ ,  $\text{Al}_2\text{O}_3$  and the  $\text{Y}_2\text{O}_3$ <sup>11,12</sup> was reported to be around  $\sim 1300^\circ\text{C}$ . As shown in Fig. 1(b) where the typical densification progress of the  $\alpha$ -SiAlON material is described, the first shrinkage rate maximum is consistent with this eutectic temperature for both Y- and Yb-doped  $\alpha$ -SiAlON. The second maximum at  $\sim 1500^\circ\text{C}$  corresponds to the dissolution of the nitride powders and the simultaneous formation of  $\alpha$ -SiAlONs.<sup>11,12,23</sup>

The original surfaces of the  $\alpha$ -SiAlON couples before joining are very rough due to the severe grinding. The plastic deformation around  $1600$ – $1700^\circ\text{C}$  in Fig. 1(a) helps to reduce the surface asperities and to heal abrasive damages<sup>7</sup> by rearranging the protruding grains and simultaneously relocating the surrounding eutectic liquid under the SPS pressure. This process consequently increases the contact of the SiAlON pieces to favor the rare earth diffusion across the interface and therefore benefit the joint formation. The total height of the joined SiAlON couples is reduced about  $\sim 0.1$  mm. This slight shrinkage can be seen in Fig. 1(a). However the  $0.1$  mm free small space between the SiAlON couples and the graphite die is not filled by the barely noticeable deformation of the SiAlON couples. This suggests the insignificance of the deformation under the  $20$  MPa joining pressure. A typical visual inspection of the joints is shown in Fig. 2. The luster of the machined surfaces of the parent sam-

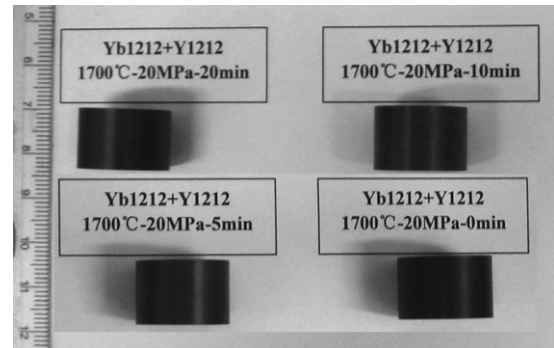


Fig. 2. Photographs of some SiAlON joints.

ples survives the high joining temperatures. No cracks or other defects relevant to the recorded deformation were observed by the naked eye.

### 3.2. Characterization

The SiAlON pieces before and after the various joining runs shared the same phase components because the chosen  $m = 1.2$ ,  $n = 1.2$  composition are thermo-dynamically stable at the temperatures from  $1600$  to  $1750^\circ\text{C}$  without possible  $\alpha \rightarrow \beta$ -SiAlON adverse phase transformation.<sup>16</sup> The typical X-ray diffraction patterns of both  $\alpha$ -SiAlON ceramics before and after the  $1700^\circ\text{C}/20$  min joining process are shown in Fig. 3. Single  $\alpha$ -SiAlON dominates the phase components before and after joining except for trace YAG in the Y-doped  $\alpha$ -SiAlON. The small increase in YAG phase content after the joining run results from the devitrification of the intergranular phases<sup>11,24</sup> for the annealing effects of the high temperatures. Lattice parameter calculation<sup>25</sup> indicates that all the  $\alpha$ -SiAlONs have  $m = 1.18$ , somewhat lower than the designated  $m = 1.2$  value. This can be attributed to and also suggests the existence of the inevitable intergranular phases.

Fig. 4 shows micrographs of the  $\alpha$ -SiAlON grain morphologies exposed by etching off the intergranular phases of the  $\alpha$ -SiAlON ceramics in molten NaOH for  $2$  min.<sup>14</sup> The SiAlON couples before and after the various joining runs have no significant differences in their microstructures. This can be

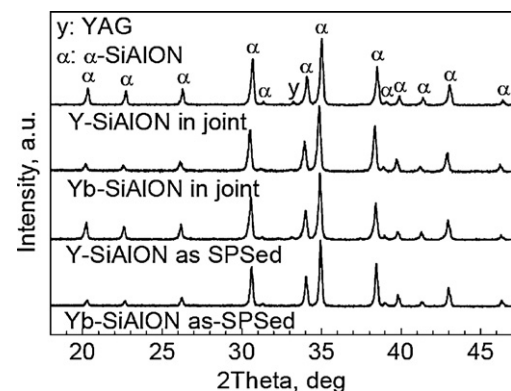


Fig. 3. XRD spectra of the  $\alpha$ -SiAlON ceramics before and after  $1700^\circ\text{C}/20$  min joining.



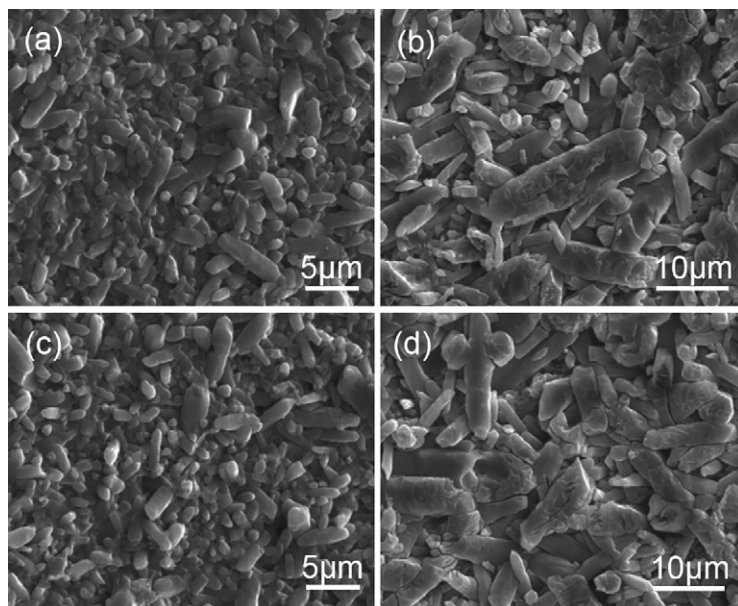


Fig. 4. Micrographs of the Yb-SiAlON (a and c) and Y-SiAlON (b and d). (c and d) Before and (a and b) after joining at 1700 °C for 20 min.

explained by the fact that the short joining time ( $\leq 20$  min) cannot significantly change the rigid skeleton of the self-toughening microstructures<sup>18</sup> of the  $\alpha$ -SiAlON ceramics either by slow Ostwald ripening or by grain orientation to form texture.<sup>21</sup>

The polished surfaces of the joints were observed by back-scattered electron imaging and some typical results are shown in Fig. 5. Due to the heavier atomic mass of the Yb species, the Yb-SiAlON shows distinct brighter contrast than the Y-SiAlON counterpart. Blocky agglomerates are present at the interfaces in the 1650 °C/10 min and the 1700 °C/0 min joints but are completely absorbed after holding for a longer time, resulting in perfect seamless joints.<sup>14</sup> The EDS analysis results in Fig. 6 show the  $\text{Si}^{4+}$ ,  $\text{Al}^{3+}$ ,  $\text{O}^{2-}$ , and  $\text{N}^{3-}$  ion constituents in these aggregations are the same as the intergranular phases in any  $\alpha$ -SiAlON ceramics.<sup>1</sup> But both Yb and Y instead of single rare earth Yb or Y have been revealed. Apparently, these agglomer-

ates acknowledge that the interfacial roughness is initially filled by a liquid. The grain rearrangement in association with the slight deformation of the SiAlON couples shown in Fig. 1(a) may squeeze the intergranular liquids to fill the vacancy between the rough contact of the parent SiAlONs to form these aggregations.

Disappearance of these aggregations is exhibited in Fig. 5(c) and (d). This is partly attributable to the liquid relocation squeezed by the local grain rearrangement under the SPS pressing. However, as soon as these grains have posited their places to balance the exerted pressure and thus stopped moving, large scale flow of the intergranular liquids becomes constrained for the lack of a sufficient driving force. The subsequent mass transportation is presumably dominated by the rare earth diffusion. In this second step,  $\text{RE}^{3+}$  should dominate diffusion because that the intergranular phases in the Y- and Yb- $\alpha$ -SiAlONs across the jointing interface have the same  $\text{Si}^{4+}$ ,  $\text{Al}^{3+}$ ,  $\text{O}^{2-}$ ,  $\text{N}^{3-}$ , and  $\text{RE}^{3+}$

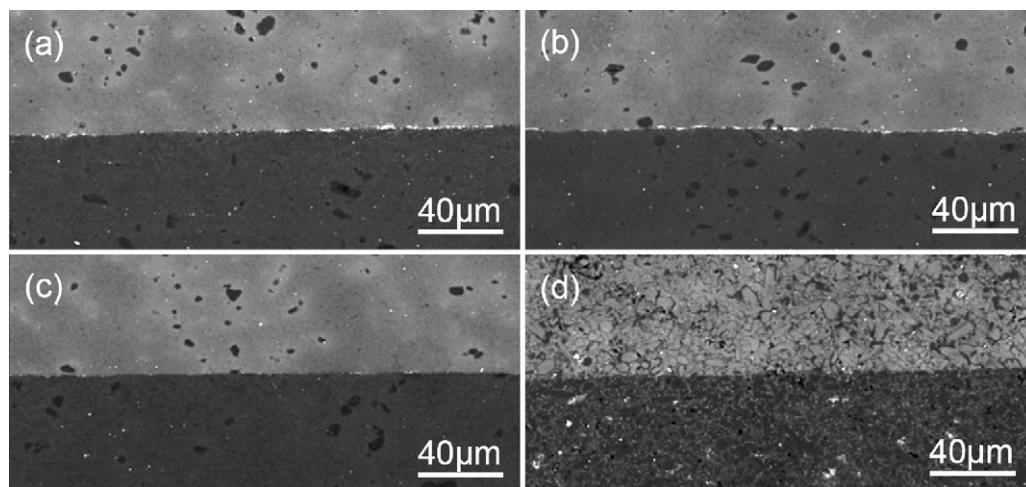


Fig. 5. Back-scattered electron images of the SiAlON joints after different joining runs (a) 1650 °C/10 min, (b) 1700 °C without holding, (c) 1700 °C/5 min, and (d) 1700 °C/10 min and further heat treatment at 1700 °C for 120 min.

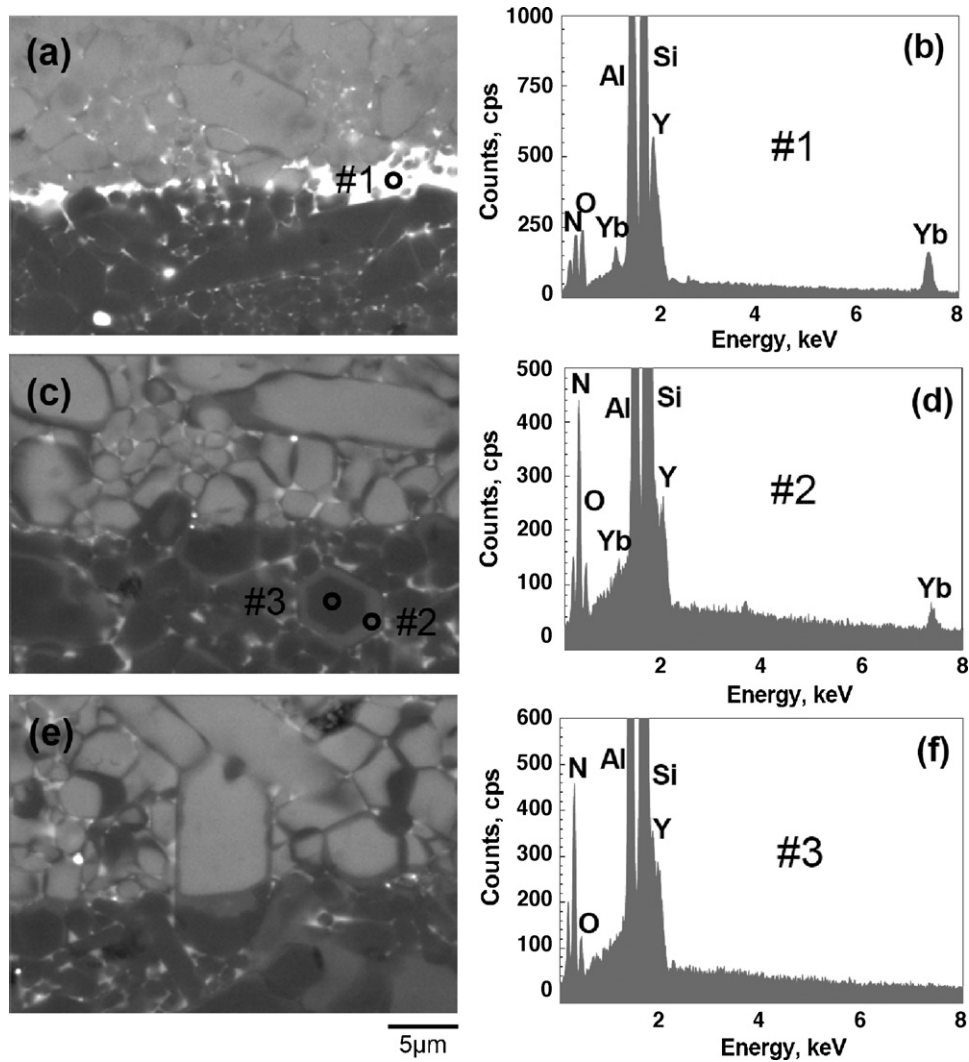


Fig. 6. Micrographs (a, c and e) and EDX spectra (b, d and f) of the different joints: (a) 1650 °C/10 min, (c) 1700 °C/20 min, and (e) 1700 °C/10 min and heat treatment at 1700 °C for 120 min; (b, d, and f) are the DEX from point #1, #2 and #3 respectively.

ion concentrations except for the different rare earth types. So the  $Y^{3+}$  and  $Yb^{3+}$  have large diffusion rates and in comparison the diffusion rates for other ions are negligible.

Fig. 6(c) and (e) shows layered structure in the  $\alpha$ -SiAlON grains in the back-scattered electron images.<sup>13,14</sup> The initial

light grey Yb-SiAlON and the dark Y-SiAlON grains are surrounded by an epitaxial layer of different contrasts, indicating different compositions. The EDX in Fig. 6(d) and (f) demonstrate an Yb/Y co-doped  $\alpha$ -SiAlON layer epitaxially grown on a Y- $\alpha$ -SiAlON core. This is because the inter-diffusion of the

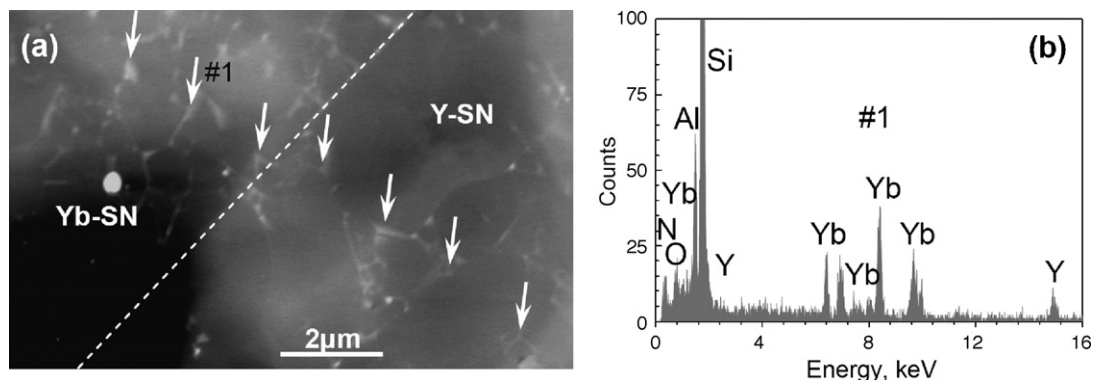


Fig. 7. STEM micrograph (a) of the SiAlON joint obtained at 1700 °C/20 min, and (b) the EDX of point #1 in (a) showing the presence of both Y and Yb in the intergranular phase of Yb-SiAlON side.

$\text{Yb}^{3+}$  and  $\text{Y}^{3+}$  across the joint interface substitutes an  $\text{Yb}^{3+}/\text{Y}^{3+}$  dual-rare earth content for the (either  $\text{Yb}^{3+}$  or  $\text{Y}^{3+}$ ) single rare earth in the intergranular phase near the joint interface. The epitaxially grown  $\alpha$ -SiAlON grains prefer picking up both  $\text{Yb}^{3+}$  and  $\text{Y}^{3+}$  rather than picking either single  $\text{Yb}^{3+}$  or  $\text{Y}^{3+}$ , forming a hybrid  $\alpha$ -SiAlON rim around the pre-existent single rare earth doped  $\alpha$ -SiAlON grain to present the clear core/shell structures that show different contrasts. This epitaxial growth of the hybrid  $\text{Yb}/\text{Y}-\alpha$ -SiAlON layer is also shown at the joint interface in Fig. 6(e) where restoration of the  $\text{Yb}$ -SiAlON grain broken by the severe pre-joining grinding extends the  $\alpha$ -SiAlON grain across the joint interface into the  $\text{Y}$ -SiAlON side. The contrast gradients may suggest possible  $\text{Yb}^{3+}/\text{Y}^{3+}$  concentration shifts at the local position with the heat treating time.

The  $\text{Yb}^{3+}$  and  $\text{Y}^{3+}$  species in the intergranular phases was also traced by an EDX with higher precision using STEM. The sophisticated STEM equipment allows an extremely narrow electron beam  $<10\text{ nm}$  to be focused on the intergranular pockets to guarantee that the EDX signals are from the local intergranular phases, thus exclude the influences of the nearby SiAlON grains. The compositions of the intergranular phases are detected along traverses perpendicular to the joint interfaces with steps  $<3\text{ }\mu\text{m}$ . This analysis process is exemplared by the arrows in Fig. 7. Fortunately the joint interface as shown by the dotted line is easily recognized due to the different grain sizes of the  $\text{Y}$ - and  $\text{Yb}$ -doped  $\alpha$ -SiAlON (see Fig. 4). The EDX spectrum in Fig. 7(b) shows peaks unambiguously attributed to  $\text{Al}^{3+}$ ,  $\text{Si}^{4+}$ ,  $\text{O}^{2-}$ ,  $\text{N}^{3-}$ ,  $\text{Y}^{3+}$  and  $\text{Yb}^{3+}$ . The extension of the  $\text{Y}^{3+}$  concentration profile into the  $\text{Yb}$ -SiAlON halves reaches  $\sim 70\text{ }\mu\text{m}$ , and increases with the increase of the soaking temperatures and times.<sup>8,14</sup> And  $\text{Yb}^{3+}$  showed the similar concentration profile. The pulsed direct current of the SPS may influence the motion<sup>21</sup> of the charged  $\text{Y}^{3+}$  and  $\text{Yb}^{3+}$  pieces. The relevant diffusion coefficients and activation energies of  $\text{Y}^{3+}$  and  $\text{Yb}^{3+}$  are under investigation and will be published elsewhere.

### 3.3. Mechanical properties

The flexure strength of  $524 \pm 42$  and  $515 \pm 39\text{ MPa}$ , fracture toughness of  $\sim 5.7 \pm 0.7$  and  $6.1 \pm 0.6\text{ MPa m}^{1/2}$ , and hardness  $19.6 \pm 0.3$  and  $19.3 \pm 0.3\text{ GPa}$ , ( $H_{V10}$ ) for the as-sintered  $\text{Yb}$ - and  $\text{Y}$ -SiAlON respectively are typical for self-toughening  $\alpha$ -SiAlON materials.<sup>12,26,27</sup> However, the strengths of  $\sim 520\text{ MPa}$  is inferior to the hot-pressed self-reinforcing  $\alpha$ -SiAlONs<sup>27</sup> having a similar microstructure as in Fig. 4, suggesting larger inhomogeneities or residual pores as microstructure defects. Obviously, decrease in the sizes<sup>9</sup> of these inhomogeneities by the slight joining deformation may have improved the flexure strength of the materials.

SPS at  $1600\text{ }^\circ\text{C}$  could not join the  $\alpha$ -SiAlON sufficiently and the flexural strength of the  $\alpha$ -SiAlON joints formed at  $1600\text{ }^\circ\text{C}$  for 20 min was only  $73 \pm 29\text{ MPa}$ . The flexural strength of the other joints is shown in Fig. 8. Once effective joints are engendered, the  $\alpha$ -SiAlON joints have strength somewhat larger than both the  $\text{Y}$ - and the  $\text{Yb}$ -SiAlON parent materials. For example the joint obtained at  $1650\text{ }^\circ\text{C}$  for 0 min had a bending strength of

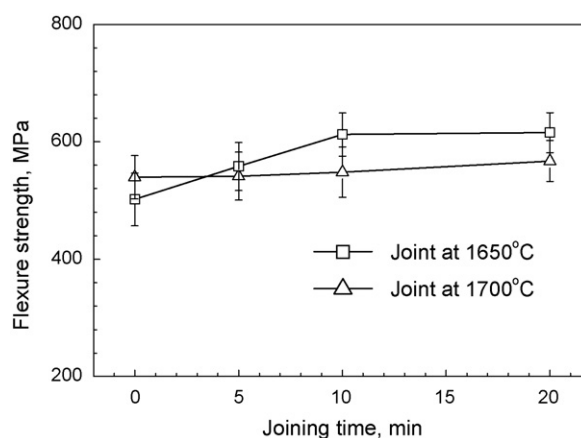


Fig. 8. Flexural strength of the joints as a function of the bonding temperatures and times.

$501\text{ MPa}$ , approaching the parent  $\text{Y}$ -SiAlON. The high flexure strength is partly attributed to the zero thermal residual stresses between the two  $\alpha$ -SiAlON materials for their similar thermal expansion coefficients.<sup>3</sup>

Fig. 8 shows that joints formed at  $1650\text{ }^\circ\text{C}$  have bending strengths increasing linearly with the holding times until reaching plateau after 10 min.<sup>7,10</sup> However when  $1700\text{ }^\circ\text{C}$  is applied, the joints formed for different joining times (from 0 to 20 min) have the steady bending strengths around  $540\text{ MPa}$ . The small strength fluctuation in these joints is within the measurement uncertainties, suggesting that the joining time in which the strength reaches plateau is reduced to 0 min using the higher joining temperature such as  $1700\text{ }^\circ\text{C}$ . Fig. 8 also shows the joint strength plateaus are higher than the as-SPS-ed parent materials. However, this strength increase cannot be resulted from the hardening effects such as orientation of the elongated  $\alpha$ -SiAlON grains because the microstructure change after the diffusion joining is essentially negligible and the strain of the SiAlON couples ( $<0.5\%$ , see Fig. 1) is too small to allow orientation texturing. Actually measuring the joint bonding strength is not an easy job because fracture always happens in either side of the parent materials. The possible flexure strength increase of the parent materials may account for the higher testing results.

The joints formed at  $1650\text{ }^\circ\text{C}$  have higher average strength than the joints formed at  $1700\text{ }^\circ\text{C}$ . This may be associated with the evolution of the intergranular phase. Becher et al.<sup>28</sup> and Guo et al.<sup>29</sup> have shown that the mechanical properties of the silicon nitride ceramics subtly depend on the interface structures between the silicon nitride grains and the surrounding intergranular phases. The intergranular phase composition changes are reasonably expected in the  $\alpha$ -SiAlONs by the annealing effects of the different joining temperatures.

Overall, the  $\alpha$ -SiAlON joints show very good mechanical properties in comparison with the as-SPS-ed materials. This good mechanical property is further evidenced by the fractographs in Fig. 9. In the fracture initiation, no evidence of joint debonding is found. The cracks initiate in one side of the parent SiAlON materials, propagate across the joining interfaces, and then break the joints. This means that the joints have at least the same level of mechanical strength as the parent mate-



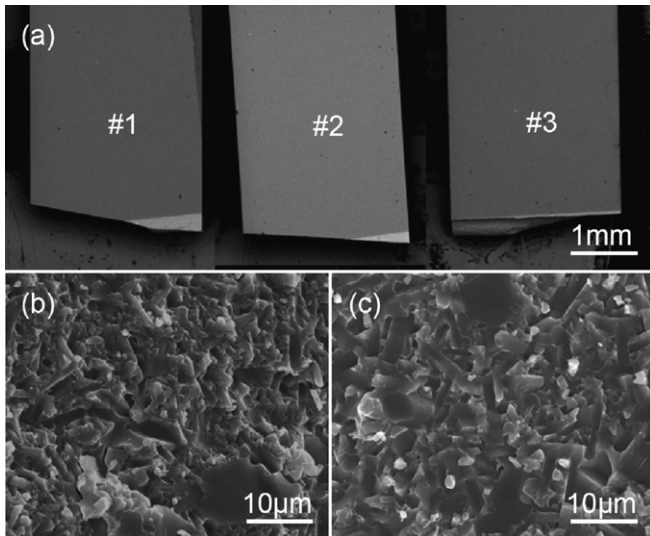


Fig. 9. Fractographs of the SiAlON joints by different SPS joining runs (a #1) 1700 °C/0 min, (a #2) 1700 °C/20 min, (a #3) 1700 °C/10 min and heat treatment at 1700 °C for 120 min, and (b) the fracture region in Yb-SiAlON and (c) the Y-SiAlON respectively in (a #1).

rials. The propagation of the cracks results in rough fractures as shown in Fig. 9(b) and (c) where bridging and friction pull-out of the elongated grains are evidenced. The interfaces between the SiAlON grains and the intergranular phases debond under the stress concentration at the crack advances to deflect the crack, thus producing the toughening mechanisms to give the good mechanical performance of the materials.

#### 4. Conclusions

In this investigation we attempted to bond  $\alpha$ -SiAlON ceramics without using any interlayer materials in a spark plasma sintering equipment. High quality joints could be formed in a few minutes by the mass transportation in the intergranular phases after being activated by sufficiently high temperatures. The intergranular liquids at the high bonding temperatures provided the diffusive paths for the various species. The joints free from residual thermal stresses show high flexure strengths reaching those of the parent materials. The modified joint microstructures by the intergrowth of the SiAlON grains across the joint interfaces also account for the good bonding strength.

#### Acknowledgements

Financial support for this work came from the Chinese Natural Science Foundation under Grant Nos. 50632020 and 90716022, and the China Postdoctoral Science Foundation under Grant No. 20090450957.

#### References

- Ekström T, Nygren M. SiAlON ceramics. *J Am Ceram Soc* 1992;**75**:259–76.
- Riley FL. Silicon nitride and related materials. *J Am Ceram Soc* 2000;**83**:245–65.

- Abed A, Hussain P, Jalham IS, Hendry A. Joining of SiAlON ceramics by a stainless steel interlayer. *J Eur Ceram Soc* 2001;**21**:2803–9.
- Esposito L, Bellosi A, Celotti G. Silicon nitride nickel joints through diffusion bonding. *Acta Mater* 1997;**45**:5087–97.
- Ceccone G, Nicholas MG, Peteves SD, Tomsia AP, Dalgeish BJ, Glaeser AM. Evaluation of the partial transient liquid phase bonding of Si<sub>3</sub>N<sub>4</sub> using Au coated Ni-22Cr foils. *Acta Mater* 1996;**44**:657–67.
- Lemus-Ruiz J, León-Patiño CA, Drew RL. Self-joining of Si<sub>3</sub>N<sub>4</sub> using metal interlayers. *Metall Mater Trans A* 2006;**37**:69–75.
- Akselsen OM. Review diffusion bonding of ceramics. *J Mater Sci* 1992;**27**:569–79.
- Glass SJ, Mahoney FM, Quillan B, Pollinger JP, Loehman RE. Refractory oxynitride joints in silicon nitride. *Acta Mater* 1998;**46**:2393–9.
- Weldon LM, Hampshire S, Pomeroy MJ. Joining of ceramics using oxide and oxynitride glasses in the Y-sialon system. *J Eur Ceram Soc* 1997;**17**:1941–7.
- Xie RJ, Mitomo M, Zhan GD, Huang LP, Fu XR. Diffusion bonding of silicon nitride using a superplastic  $\beta$ -SiAlON interlayer. *J Am Ceram Soc* 2001;**84**:471–3.
- Bandyopadhyay S, Hoffmann MJ, Petzow G. Desiccation behavior and properties of Y<sub>2</sub>O<sub>3</sub>-containing  $\alpha$ -SiAlON-based composites. *J Am Ceram Soc* 1996;**79**:1537–45.
- Kurama S, Herrmann M, Mandal H. The effect of processing conditions, amount of additives and composition on the microstructures and mechanical properties of  $\alpha$ -SiAlON ceramics. *J Eur Ceram Soc* 2002;**22**: 109–19.
- Gopal M, Jonghe LD, Thomas G. Silicon nitride: from sintering to joining. *Acta Mater* 1998;**46**:2401–5.
- Gopal M, Sixta M, Jonghe LD, Thomas G. Seamless joining of silicon nitride ceramics. *J Am Ceram Soc* 2001;**84**:708–12.
- Omori M. Sintering, consolidation, reaction and crystal growth by the spark plasma system (SPS). *Mater Sci Eng A* 2000;**287**:183–8.
- Rosenflanz A, Chen IW. Phase relationships and stability of  $\alpha$ -SiAlON. *J Am Ceram Soc* 1999;**82**:1025–36.
- Anstis GR, Chantikul P, Lawn BR, Marshall DB. A critical evaluation of indentation techniques for measuring fracture toughness. *J Am Ceram Soc* 1981;**64**:533–8.
- Shen Z, Zhao Z, Peng H. Formation of tough interlocking micro-structures in silicon nitride ceramics by dynamic ripening. *Nature* 2002;**417**: 266–9.
- Meléndez JJ, Rodríguez AD. Creep of silicon nitride. *Prog Mater Sci* 2004;**49**:19–07.
- Meléndez JJ, Melendo JM, Rodríguez AD, Wötting G. Creep behaviour of two sintered silicon nitride ceramics. *J Eur Ceram Soc* 2002;**22**: 2495–9.
- Shen Z, Peng H, Nygren M. Formidable increase in superplasticity of ceramics in the presence of an electric field. *Adv Mater* 2003;**15**:1006–9.
- Chihara K, Hiratsuka D, Tatami J, Wakai F, Komeya K. High-temperature deformation of  $\alpha$ -SiAlON nanoceramics without additives. *Scripta Mater* 2007;**56**:871–4.
- Menon M, Chen IW. Reaction densification of  $\alpha$ -SiAlON: II, densification behavior. *J Am Ceram Soc* 1995;**78**:553–9.
- Ye F, Hoffmann MJ, Holzer S, Zhou Y, Iwasa M. Effect of the amount of additives and post-heat treatment on the microstructure and mechanical properties of yttrium- $\alpha$ -sialon ceramics. *J Am Ceram Soc* 2003;**86**:2136–42.
- Herrmann M, Kurama S, Mandal H. Investigation of the phase composition and stability of the  $\alpha$ -SiAlONs by the Rietveld method. *J Eur Ceram Soc* 2002;**22**:2997–3005.
- Zenotchkine M, Shuba R, Chen IW. Effect of seeding on the microstructure and mechanical properties of  $\alpha$ -SiAlON: III, comparison of modifying cations. *J Am Ceram Soc* 2003;**86**:1168–75.
- Zenotchkine M, Shuba R, Kim JS, Chen IW. Effect of seeding on the microstructure and mechanical properties of  $\alpha$ -SiAlON: I, Y-SiAlON. *J Am Ceram Soc* 2002;**85**:1254–9.
- Becher PF, Sun EY, Hsueh CH, Alexander KB, Hwang SL, Waters SB, et al. Debonding of interfaces between beta-Silicon nitride whiskers and Si–Al–Y oxynitride glasses. *Acta Mater* 1996;**44**:3881–93.
- Guo G, Li J, Yang X, Lin H, Liang L, He M, et al. Direct measurement of residual stresses and their effects on the microstructure and mechanical properties of heat-treated Si<sub>3</sub>N<sub>4</sub> ceramics. *Acta Mater* 2006;**54**:2311–6.